TECHNICAL NOTE

EXPERIMENTAL STUDY OF THE INTERACTION OF CORROSION DAMAGE AND OUT-OF-CIRCULARITY IN THE COLLAPSE OF SUBMARINE PRESSURE HULLS

(DOI No: 10.3940/rina.ijme.2012.a3.229tn)

J R MacKay and **M J Smith**, Defence R&D Canada – Atlantic, Canada
F van Keulen and **T N Bosman**, Delft University of Technology, The Netherlands

SUMMARY

The effect of corrosion damage on overall collapse strength of submarine pressure hulls was studied experimentally. Ring-stiffened cylinders were machined from aluminium tubing and loaded to collapse under external pressure. In selected specimens, some of the outer shell material was machined away in large single patches, representing general corrosion. Other specimens had many smaller patches, representing corrosion pitting from the outside of the hull, followed by grinding. Large-amplitude out-of-circularity (OOC) was introduced by mechanically deforming selected cylinders. Clusters of artificial corrosion pits were found to have approximately the same effect on collapse pressure as equal-depth general corrosion covering the same region of plating. General corrosion was found to be most severe when it was "in-phase" with OOC, since, during pressure loading, high compressive stresses resulting from corrosion were compounded by compressive bending stresses associated with OOC, and furthermore, the corrosion tended to increase the geometric imperfection itself. On the other hand, out-of-phase corrosion reduced the effect of OOC, while at the same time the thinning-associated compressive stresses were counteracted by local tensile bending stresses associated with OOC, so that strength reductions were correspondingly smaller. Overall collapse pressures for corroded specimens were reduced by, on average, 0.85% for each 1% of shell thinning. That result is based on a linear approximation of the nonlinear relationship between thinning and collapse pressure. The linear trend-line, which was used to account for the experimental scatter, is based on specimens with 13 to 27% shell thinning, and with a variety of corrosion areas and OOC amplitudes.

NOMENCLATURE

a	nominal mid-plane shell radius (mm)
e_{max}	maximum measured radial eccentricity (mm)
h	mean measured shell thickness (mm)
m	number of half sine waves over the length of a cylinder
n	number of complete waves about the circumference of a cylinder
P_b	boiler pressure (MPa)
P_c	experimental collapse pressure (MPa)
P_c*	normalized experimental collapse pressure (-)
δ_c	maximum measured shell thinning (%)
λ_c	corrosion knock-down factor
σ_y	mean measured 0.2% yield stress in the circumferential direction (MPa)

1. INTRODUCTION

The critical structural component of a naval submarine, with respect to life-cycle management (LCM), is its pressure hull. This is due to its importance for safe diving operations, the sensitivity of its structural capacity to defects and damage, and the high cost of repairing or replacing damaged sections. The life-cycle of a pressure hull can be limited by the accumulation of fatigue and corrosion defects, and by structural damage resulting from weapons loads or collision. The current paper is only concerned with corrosion aspects of LCM.

Hull corrosion can be prevented by using preservatives or impressed current cathodic protection. Nonetheless, it still occurs in practice [1], in either of two forms. With general corrosion, the hull surface is affected approximately uniformly over a large area, and the damage is typically shallow compared to the hull thickness. General corrosion at 10% of the hull thickness would be considered severe. On the other hand, corrosion pitting can penetrate deep into the hull, sometimes through as much as half the thickness, but may be just a fraction of the hull thickness in diameter.

Both types of damage are treated by grinding away the corroded material, leaving a hull with locally reduced thickness. In the case of pitting damage, the affected area may be much larger after grinding due to the size of the grinding wheel and attempts to blend or fair the damaged region with the intact hull. Furthermore, while the highly localized nature of corrosion pitting may mean that a single ground-out pit has a negligible impact on hull strength, closely spaced pits may interact so that the net effect of a cluster of pits is potentially significant.

Hull thickness can be restored using weld overlay, but that procedure is expensive and its secondary effects, including residual stresses, distortions, and changes in material properties, are still being studied [2]. So, in certain circumstances it is preferable to operate the submarine with a hull thickness that has been reduced by corrosion damage.

Conventional design codes allow for only a small amount of corrosion thinning, if any at all [3], mainly because there is a considerable weight penalty to be paid when a general hull wastage allowance is factored into the design. The structural capacity of an in-service hull with an out-of-tolerance case of corrosion is typically assessed by assuming that the entire hull has been uniformly thinned. That conservatism compensates for the uncertainty associated with the effect of a given type and extent of corrosion damage. As a result, cases of ground-out but otherwise unrepaired corrosion damage often require a reduction to the submarine's deep diving depth in order to maintain acceptable safety margins [1,3,4].

The conservatism associated with general corrosion tolerances can be addressed by studying the effect of more realistic, discrete patches of corrosion damage on hull strength. That type of damage was studied experimentally in [5], whereby general corrosion was applied to aluminium ring-stiffened cylinders by machining away some of the shell material in rectangular patches of uniform depth. The axisymmetric geometry of some of those specimens is shown in Figure 1. The experiments studied the effect of corrosion on overall collapse, characterized by elasto-plastic buckling of the combined shell plating and ring-stiffeners, as well as interframe collapse resulting from inelastic buckling of the shell between stiffeners.

In [5], corrosion damage was found to reduce cylinder collapse strength through early yielding brought on by high stresses in the corroded area. The increased stresses were attributed to higher membrane and bending stresses due to the thinner shell and to additional bending stresses that arose due to the shell eccentricity associated with one-sided thinning. Comparisons between undamaged and corroded test specimens showed a strong correlation between corrosion thinning and the percentage reduction to overall collapse pressure, which was found to be approximately equal to the percentage shell thinning. General corrosion was found to have a much smaller effect on interframe collapse, compared with overall collapse. Heavy ring-stiffeners in specimens failing by interframe collapse provided some reserve strength after the corroded shell had failed locally. That reserve strength was not available with the lighter ring-stiffeners in overall collapse specimens.

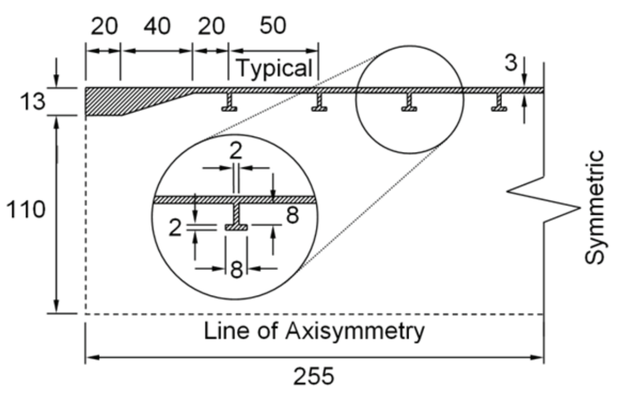

Figure 1: Nominal axisymmetric geometry of the test specimens. All dimensions are in millimetres.

In [6], the experimental study from [5] was extended to examine the effects of material properties on the strength of damaged hulls by comparing cylinders fabricated from two grades of aluminium. As expected, cylinder collapse strength was found to be sensitive to yield strength. More interestingly, the effect of corrosion damage was found to be related to the degree of strain hardening. Test specimens made from aluminium with a relatively greater strain hardening modulus were less affected by a given corrosion case.

The interaction of general corrosion damage with out-of-circularity (OOC) in hulls failing by overall collapse was studied numerically in [7]. In that paper, Kendrick's finite difference method for determining overall collapse pressures [8] was modified to allow discrete patches of corrosion wastage to be modelled. It was found that the effects of corrosion thinning are not limited to the reduction of the overall bending stiffness of the hull. The load-path eccentricity that results from one-sided thinning effectively increases or decreases the OOC magnitude depending on whether the corrosion is collocated with an inward ("in-phase") or an outward ("out-of-phase") OOC lobe, respectively. That leads to a nonlinear interaction between corrosion and OOC, whereby the effect of a given level of in-phase shell thinning was found to diminish with increasing OOC magnitudes. That was attributed to the relatively smaller OOC-like effect of corrosion when initial imperfections were of greater magnitude.

The analyses in [7] also indicate that overall collapse pressures are markedly more affected by in-phase corrosion compared with out-of-phase corrosion. With in-phase cases, the imperfections introduced by corrosion and OOC are additive, and, under pressure loading, the high compressive stresses that arise at the corrosion due to the thinning itself are compounded by compressive bending stresses associated with OOC. Out-of-phase corrosion reduces the OOC imperfection, and the positioning of the corrosion where the bending stresses associated with OOC are in tension tends to counteract the high compressive stresses that arise in the thinned shell. In some cases, out-of-phase corrosion was found to improve the OOC shape, and the stress field under loading, to an extent that the collapse pressure was greater than a similar model with no corrosion.

The test specimens in [5,6] were produced by machining, so that, other than the corrosion defects, they were nearly shape-perfect. That allowed the effect of corrosion damage to be studied in isolation from other shape defects, but the interaction between OOC and corrosion that was predicted in [7] could not be verified. Furthermore, the earlier experiments were focused on large areas of general corrosion damage, and corrosion pitting was not studied.

The current paper extends the experiments in [5,6] to cylinders with more realistic levels of OOC and types of corrosion. Large-amplitude OOC was introduced by mechanically deforming as-machined cylinders with and without general corrosion damage. The current tests also examine the effect of clusters of corrosion pits that have been treated by grinding only. The current work is concerned with overall elasto-plastic collapse, since OOC has the greatest impact on that failure mode, and since interframe collapse pressures in [5] were shown to be less sensitive to corrosion damage. The nominal geometry of the current test specimens is shown in Figure 1 and photographs of some typical specimens are shown Figure 2.

The overall goal of the work presented in [5,6] and the current research is to overcome the uncertainty associated with hull corrosion and its effect on collapse strength in order to reduce the conservatism of current corrosion tolerances. The number of corrosion cases that can be studied experimentally is limited, but numerical models can be used to study any arbitrary pattern of thinning. With that in mind, effort has also been directed at identifying and validating numerical procedures for predicting the effects of corrosion damage, so that numerical models can be used to make assessments of damaged submarine hulls. That work is presented in [9], where the experimental results from [5] were used to validate nonlinear finite element (FE) collapse predictions. The current paper deals only with experiments.

This paper begins with a description of the test specimens and experimental procedures in Section 2. The experimental results are presented in Section 3. The interaction of corrosion and OOC is discussed in Section 4, along with a comparison between general corrosion and pitting damage, and a summary of the entire testing program including results from [5,6]. Conclusions are presented in Section 5.

2. TEST SPECIMENS AND PROCEDURES

The sixteen cylinder specimens considered here are listed in Table 1 and Table 2. Table 1 shows the type of corrosion damage, and the measured shell thinning (δ_c), OOC magnitude, circumferential yield stress (σ_y), and collapse pressure (P_c) for specimens with large-amplitude OOC. Specimens without corrosion damage are referred to as "intact" cylinders. Table 2 presents the same data for as-machined specimens with corrosion pitting. The various cases of corrosion damage are described in Table 3. The test specimens and procedures are briefly described in the following sections. The reader is referred to the experimental reports in [10,11] for greater detail.

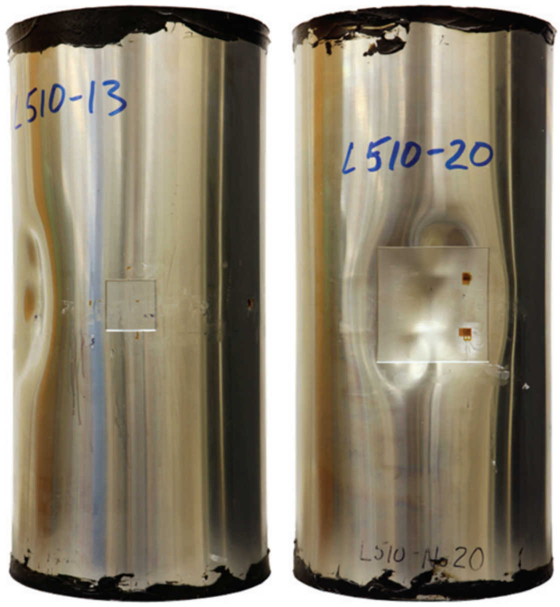

(a) Cylinders with large-amplitude out-of-circularity and general corrosion damage, shown after testing. L510-No13, with out-of-phase Patch B corrosion, is shown on the left. The right-hand cylinder is L510-No20, with in-phase Patch C corrosion.

(b) L510-No24, with Pitting B damage (general corrosion and pitting), before testing. The pit numbering scheme is shown at the inset.

Figure 2: Photographs of typical cylinder specimens.

2.1 AXISYMMETRIC GEOMETRY

A CNC lathe was used to machine the axisymmetric geometry of each test specimen from an extruded aluminium alloy tube. The nominal dimensions of the cylinders, which are shown in Figure 1, are the same as some of the specimens from earlier experiments in [5,6].

The shell plating was proportioned to be relatively stiff compared to the T-section ring-stiffeners in order to promote failure by overall collapse. The thick end rings and tapered end bays were designed to prevent undesired end bay failures, and to provide enough material to bolt the steel end caps that were used during pressure testing.

2.2 OUT-OF-CIRCULARITY

The design collapse pressure of a pressure hull is determined by assuming that the maximum radial eccentricity, e_{max}, is equal to 0.005 times the hull radius, a, or in the common terminology, 0.5% [3]. Overall collapse pressures are calculated for a range of circumferential wave numbers, n, and the most pessimistic prediction is used for design. It is assumed that the most pessimistic axial mode is a half sine wave over the length of the hull, or m=1. Construction tolerances generally require the OOC of the as-built hull to be less than one-third of the design value, or approximately 0.17% [3]. That allows for growth of OOC during the life of the hull.

In the current study, the OOC of intact cylinders was measured using a coordinate measurement machine (CMM), while laser displacement gauges mounted on a turntable were used to measure the shape of corroded specimens. Measurements were taken at 36 circumferential positions at each stiffener and mid-bay location along the cylinder length. The accuracies of the CMM and the laser displacement gauges are 0.02 and 0.001 mm, respectively. Those accuracies are equivalent to 0.016% and 0.0008% OOC, respectively.

OOC measurements of as-machined cylinders indicated that they were nearly shape-perfect, with maximum values no greater than 0.07% (see Table 2). The machining process resulted in OOC characterized by two complete waves about the circumference of each cylinder (n=2), distributed approximately uniformly over the specimen length (m=0). In contrast, the critical overall collapse mode of the cylinders is m=1, n=3 [5].

With one exception, the cylinders in Table 1 were mechanically deformed to achieve OOC in the critical m=1, n=3 mode, at magnitudes up to twice the design value of 0.5%. The exception is L510-No34, which was designed to study the effect of the axial distribution of OOC. Its intended OOC shape was characterized by an n=3 circumferential mode, and a complete sine wave along the length (m=2).

OOC was applied by deforming the cylinders using a triangular steel frame with bolted joints at its corners. Load was applied at 120° increments by tightening the bolts so that the mid-points of the triangle legs pressed against the cylinder. The desired OOC shape was built up by moving the load frame along the length of the cylinder and incrementally increasing the permanent deformations.

Table 1: Test specimens with general corrosion patches and large-amplitude OOC.

Specimen	**Corrosion[a] Patch**	**δ_c**	**OOC[b]**	**σ_y (MPa)**	**P_c (MPa)**
L510-No13	B*	21.2%	0.71%	328	7.55
L510-No14	B	23.9%	0.67%	334	6.93
L510-No17	Intact		0.39%	306	7.84
L510-No18	Intact		0.41%	305	7.71
L510-No19	C	17.4%	0.77%	329	6.67
L510-No20	C	18.6%	0.67%	325	6.93
L510-No25	Intact		0.75%	305	7.13
L510-No26	Intact		0.94%	310	7.05
L510-No33	Intact		0.92%	301	7.03
L510-No34	Intact		0.45%	301	8.02
L510-No35	B	19.0%	0.79%	332	6.58
L510-No36	B*	24.6%	0.97%	331	7.22

Note (a) An asterisk (*) denotes out-of-phase corrosion; otherwise, the corrosion damage is in-phase with OOC.
Note (b) OOC is defined as the maximum measured radial eccentricity at the outside of the cylinder, e_{max}, divided by the nominal mid-plane shell radius, a.

Table 2: Test specimens with corrosion pitting damage and as-machined OOC.

Specimen	**Pitting Type**	**δ_c**	**OOC**	**σ_y (MPa)**	**P_c (MPa)**
L510-No21	A	14.4%	0.06%	337	8.65
L510-No22	A	16.2%	0.07%	331	8.98
L510-No23	B	24.1%	0.07%	326	7.63
L510-No24	B	26.5%	0.05%	340	7.62

Table 3: Nominal corrosion damage cases.

Case	**Description[a]**
Intact	No corrosion damage
Patch B	Single 42×42×0.6 mm (20%) general corrosion patch outside shell
Patch C	Single 100×100×0.4 mm (13.3%) general corrosion patch outside shell
Pitting A	Sixteen 10×10×0.4 mm (13.3%) randomly oriented corrosion pits
Pitting B	Sixteen 10×10×0.4 mm (13.3%) randomly oriented corrosion pits superimposed on a 100×100×0.3 mm (10%) general corrosion patch (23.3% total thinning at pits)

Note: (a) Corrosion patch sizes are specified by the circumferential times the axial extents times the depth. The nominal percentage thinning is shown in parentheses. General corrosion patches and groups of corrosion pits were centred at the mid-length of the cylinders.

Graphical representations of the final pre-testing OOC for typical cylinders are shown in Figure 3. The images were generated by performing two-dimensional Fourier decompositions of the measured OOC, and applying those nonlinear maps to FE models of the specimens. The Fourier analyses confirmed that the OOC was dominated by the m=1, n=3 mode for all cylinders with that target shape. With most of those cylinders, the OOC amplitude associated with the target mode was an order of magnitude greater than the next largest contributor. In some cases, significant OOC contributions were unintentionally introduced for some higher order modes, especially m=1, n=6 and, to a lesser extent, m=n=3. Those modes are seen as interframe dimples superimposed on the more dominant m=1, n=3 mode in the models in Figure 3. It was also confirmed that the as-measured shape of L510-No34 was dominated by the m=2, n=3 mode.

2.3 CORROSION DAMAGE

Artificial corrosion damage was applied to selected cylinders by machining away some of the outer shell material in square patches of approximately uniform depth. General corrosion damage was applied to the cylinders listed in Table 1. The damage was either in-phase with OOC, whereby the corrosion patch was approximately collocated with an inward lobe of the overall OOC shape, as shown in Figure 3(a), or out-of-phase, whereby the corrosion was applied at an outward OOC lobe, as in Figure 3(b). Patch B was applied in-phase with OOC in two cases, and out-of-phase in two cases. Patch C was always applied in-phase with OOC.

Specimens in Table 2 had sixteen 10×10 mm areas of uniform corrosion, representing corrosion pits after grinding. Each pit was 20% of the frame spacing in breadth. The pits were randomly oriented within a 100×100 mm bounding area, as shown in Figure 4. Cylinders with Pitting A corrosion had only the pitting damage. With Pitting B corrosion, the pits were superimposed on general corrosion covering the bounding area. Pit positions were the same on all specimens with Pitting A and B damage.

2.4 MATERIAL PROPERTIES

The specimens were machined from extruded tubes of 6082-T6 aluminium alloy. Previous batches of that aluminium showed an anisotropy, with a yield stress in the circumferential direction that was approximately 10% less than the axial yield stress [5,6]. For the current study, tensile coupons were machined from the thick end rings of each cylinder, in the critical circumferential direction, after collapse testing. The end rings were not plastically deformed during pressure testing.

The average measured circumferential yield stress for each specimen is given in Table 1 and Table 2. The intact

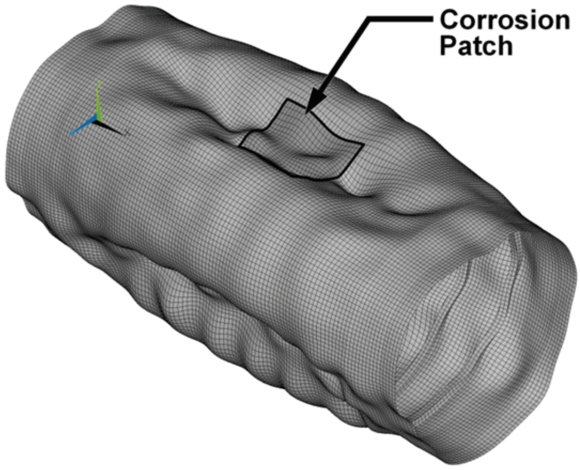

(a) L510-No19, with m=1, n=3 OOC, and in-phase corrosion.

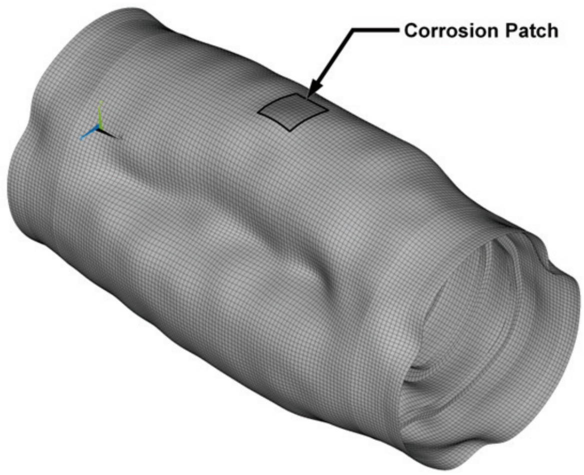

(b) L510-No36, with m=1, n=3 OOC, and out-of-phase corrosion.

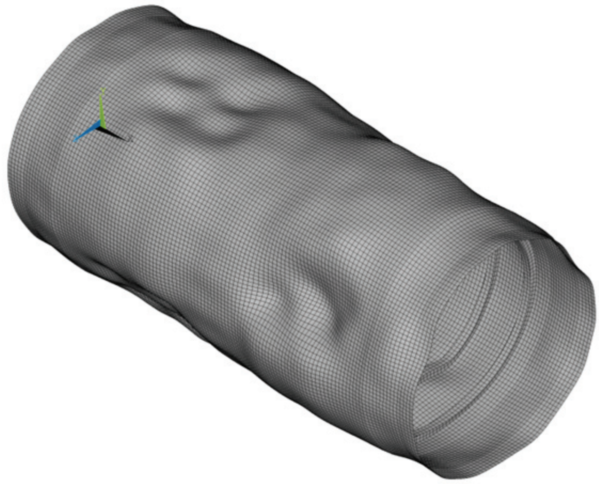

(c) L510-No34, with m=2, n=3 OOC, and no corrosion.

Figure 3: Representation of as-measured OOC, amplified by a factor of 50 for clarity, for selected specimens.

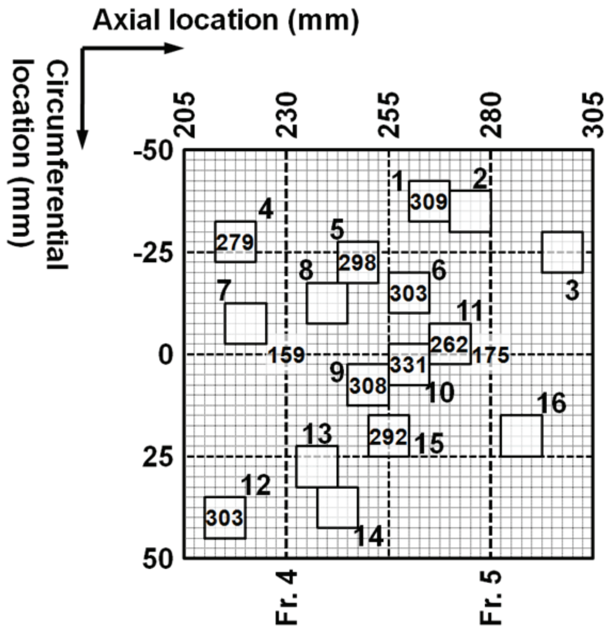

Figure 4: Corrosion pit locations and numbering. The thick outer line represents the bounding box and general corrosion patch for Pitting A and B, respectively. Numbers inside pits and at ring-stiffeners are strain-derived von Mises stresses (MPa) outside the shell of L510-No22 at a pressure of 7.13 MPa (see Section 3.2).

and corroded cylinders were machined from different batches of aluminium tubing, resulting in different yield stresses. The yield stress of the corroded group was approximately 9% greater, on average, than the intact group.

Young's modulus measurements were more consistent between batches, but the average value for all specimens was approximately 57 GPa, which is significantly lower than the typical handbook value of approximately 70 GPa [12], as well as measured values for previously tested cylinders [5,6]. It appears that a misalignment of the coupons in the load frame resulted in unintentional bending stresses. Since only one extensometer was used during tensile testing, the bending stresses could not be factored out of Young's modulus calculations. All calculations in this paper that require Young's modulus use the handbook value of 70 GPa.

Poisson's ratio was not measured for the current study, but measured values for previously tested cylinders that were machined from the same material were between 0.32 and 0.34 [5].

2.5 PRESSURE TESTING

Pressure testing was conducted in a pressure chamber using the so-called "volume-control" method [13], which allows violent collapse displacements to be better controlled compared to conventional air-backed pressure testing. With the volume-control approach, the specimen is filled with testing fluid and is initially pressurized from the inside and the outside. The cylinder is then loaded by regulating the internal pressure using a series of hoses and valves in order to achieve the desired net external pressure.

In the current tests, a non-conductive mineral oil was used as the pressure testing fluid. Mild steel end caps, 38 mm thick, were attached to both ends of each specimen with bolts and sealed with a polymeric compound. Each specimen was loaded until it collapsed, with the collapse pressure defined as the maximum recorded net pressure. The accuracy of the reported collapse pressures, ±0.09 MPa, is based on the pressure transducers used during testing.

Each cylinder was instrumented with 64 to 72 strain gauges. A typical intact cylinder was instrumented with strain gauges at twelve equally spaced increments about the circumference at the flanges of the two central stiffeners and outside the shell in the central bay. Cylinders with large-amplitude OOC had a row of gauges along the cylinder length to measure the axial distribution of strain outside the shell. Cylinders with artificial corrosion had additional gauges in the damaged area. Gauges fixed to the shell were 2-gauge 90° tee rosettes, aligned in the circumferential and axial directions, while uni-axial gauges were fixed to the ring-stiffener flanges in the circumferential direction. The strain measurements are accurate to within ±0.5% of the reported strain values. Strain gauge and pressure transducer readings were taken at a sampling rate of 100 Hz for all tests.

Reported yield pressures are based on the first occurrence of the von Mises equivalent stress reaching the measured circumferential yield stress. Von Mises stresses were calculated using a generalized Hooke's law with the measured circumferential and axial strains, and assuming a plane stress condition whereby the in-plane shear stresses are considered to be negligible. The procedure for calculating stresses from measured strain values is described in greater detail in [5].

3. EXPERIMENTAL RESULTS

The experimental collapse pressure for each test specimen is given in Table 1 and Table 2. All of the cylinders failed by overall collapse. Typical failure modes are shown in the post-testing photographs in Figure 2. The results for a few typical cases are presented in this section, and the general trends are examined in Section 4.

3.1 SPECIMENS WITH LARGE-AMPLITUDE OUT-OF-CIRCULARITY

The measured circumferential strain distributions indicated that all of the test specimens with large-amplitude OOC (Table 1) failed in the expected overall n=3 collapse mode. Figure 5 shows that the shell bending strains for an intact specimen follow the expected distribution with respect to the initial imperfections. The post-testing photographs in Figure 2 show post-collapse deformations concentrated at one of the three inward OOC lobes, even for cylinders with out-of-phase corrosion. Cylinders with in-phase corrosion failed at the location of shell thinning.

Figure 6 shows measured pressure-strain curves for intact and corroded specimens with similar OOC magnitudes. Shell strains were much greater at the inward OOC lobe compared to the outward lobe for the intact cylinder and the specimen with in-phase corrosion. As expected, large shell strains at the in-phase corrosion patch caused that cylinder to yield earlier than the intact specimen. There was less difference between the strain magnitudes at inward and outward OOC lobes for the cylinder with out-of-phase corrosion, because the compressive strains resulting from the corrosion damage were offset by tensile bending strains at the outward OOC lobe. That cylinder failed at an inward OOC lobe away from the shell thinning.

The pressure-strain curves in Figure 6, and the collapse pressures listed in Table 1, suggest that the cylinder with in-phase corrosion was only slightly weaker than the intact specimen. Furthermore, the cylinder with out-of-phase corrosion appears to be even stronger than the intact specimen. Those results are misleading, since the material used for the corroded specimens had a yield strength between 7.5 and 9.5% greater than that used for the intact cylinder. The effect of yield stress is dealt with in the discussion in Section 4.

3.2 SPECIMENS WITH CORROSION PITTING

The measured strain data indicate that the four cylinders with corrosion pitting failed by overall collapse in the n=3 mode. Post-collapse displacements were concentrated around the corrosion damage, as shown by the post-testing photograph of L510-No22 in Figure 7. Figure 7 also shows selected pressure-strain curves for that specimen. Strain-derived von Mises stresses at instrumented pits are shown in Figure 4. Those stresses are associated with the applied pressure at which the shell first yielded at corrosion pit no. 10.

Figure 4 and Figure 7 show that stresses and strains in the corrosion pits were significantly greater than for the intact shell. Yielding occurred first at the pits, but overall collapse was precipitated by yielding of the intact shell between pits and near the central ring-stiffeners. The shell stresses and strains were greatest at pit no. 10, which was near the centre of the damaged area, and immediately adjacent to two pits. Furthermore, pit no. 10 was situated near the centre of the frame-bay. The corrosion pit with the lowest stress and strain, pit no. 4, was located at the periphery of the damaged area, and was relatively isolated and closer to a ring-stiffener.

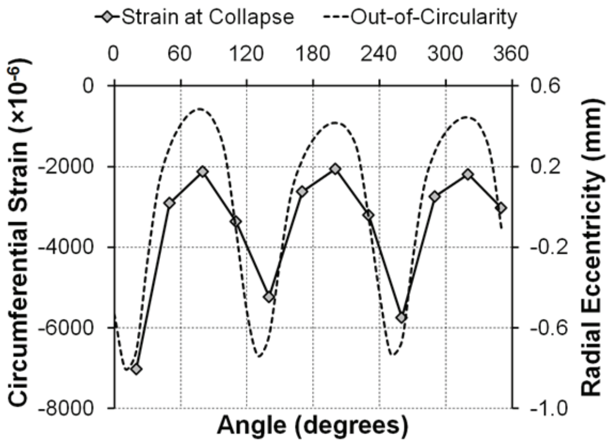

Figure 5: Circumferential distribution of shell strain outside the central bay of L510-No25 at the collapse pressure; the corresponding initial OOC is shown on the secondary vertical axis.

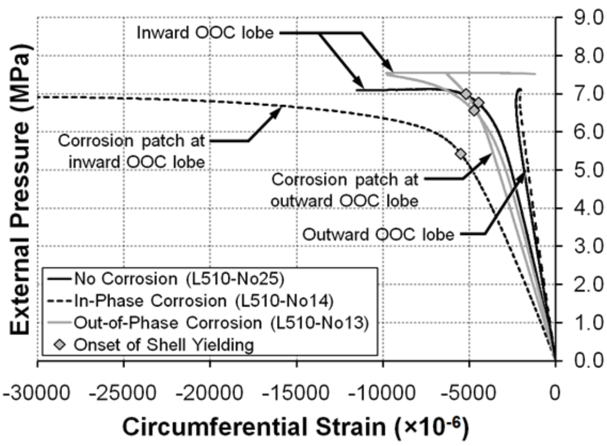

Figure 6: Pressure-strain curves for cylinders with large-amplitude OOC; showing circumferential strains measured on the outside of the shell in the central bay.

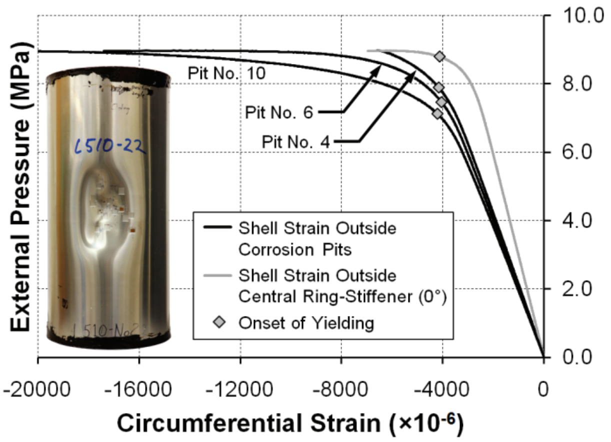

Figure 7: Selected pressure-strain curves for L510-No22 (Pitting A damage).

The responses of the other specimens with corrosion pitting were similar to L510-No22. The measured strains were greater in the cylinders with Pitting B damage due to the deeper pits and the presence of the general corrosion patch.

4. DISCUSSION

Specimen-to-specimen comparisons in [6] were made using collapse pressures that were normalized to account for differences in the circumferential yield strengths, as determined from coupon tests. The current paper adopts the same procedure, whereby the normalized collapse pressure for each specimen is taken as P_c*=P_c/P_b, where P_c is the experimental collapse pressure and P_b is the boiler pressure. The boiler formula, $P_b=\sigma_y h/a$, is a simple expression for predicting the onset of yielding in unstiffened pressure vessels. This normalization procedure neglects axial stresses, as well as the material anisotropy discussed earlier; however, FE models show that cylinder collapse pressures are governed by the circumferential material properties [9].

The current paper also adopts the procedure that was used in [6] to quantify the effect of corrosion damage on collapse strength. In that paper, a corrosion "knock-down factor", λ_c, was derived for each corroded specimen. λ_c is taken as the quotient of the normalized collapse pressures for a corroded cylinder and its intact counterpart(s).

4.1 INTERACTION OF GENERAL CORROSION WITH OUT-OF-CIRCULARITY

The mechanical application of OOC introduced residual stresses and strain hardening that could have affected the collapse strength of the cylinders. Nonetheless, the current discussion is concerned with comparing the strength of intact and corroded cylinders with similar magnitudes of OOC, and thus, similar levels of residual stresses and hardening. Therefore, those aspects of the problem are approximately factored out of cylinder-to-cylinder comparisons, and are not thought to have significantly affected the conclusions of the current study with respect to the interaction of OOC and corrosion.

Normalized experimental collapse pressures for specimens with large-amplitude OOC are plotted against the level of OOC in Figure 8. The experimental curve is based on linear least squares regression of the data for the five intact cylinders with m=1, n=3 OOC. The curve-fitting parameters for that experimental curve, as well as those for other data sets discussed below, are listed in Table 4.

Figure 8 shows that the relationship between the collapse strength of intact cylinders and OOC magnitude is approximately linear in the range considered. The strength of the intact cylinder with m=2, n=3 OOC falls above the m=1, n=3 trend-line. That can be explained in general terms by the fact that the OOC of the cylinder did not correspond with the critical m=1 axial buckling mode. More precisely, its greater strength is due to relatively smaller bending stresses that arise under pressure loading for the shorter axial wavelength associated with m=2 OOC.

All of the cylinders with general corrosion damage fall below the intact trend-line in Figure 8. As expected, there is a strong interaction between corrosion damage and OOC. With in-phase corrosion, the effects of one-sided hull thinning and imperfections were additive, which leads to significant decreases in collapse pressure. The data for cylinders with out-of-phase corrosion are much closer to the intact trend-line than the in-phase cases. That is because the bending stresses associated with OOC and corrosion for out-of-phase cases are of opposite sign and counteract each other. Furthermore, the out-of-phase damage tends to effectively reduce the level of OOC. Those factors result in smaller reductions in collapse pressures.

Figure 9 shows corrosion knock-down factors for specimens that had general corrosion damage, versus the maximum measured corrosion thinning, δ_c. That figure also shows data for specimens with pitting damage, but those results will be discussed in the next section. For as-machined specimens, λ_c was calculated by dividing P_c* for each corroded specimen by P_c* for the intact cylinder with the same axisymmetric geometry and fabricated from the same batch of material. In cases where two nominally identical intact specimens were available, the average value of P_c* was used in the λ_c calculation. The λ_c calculation for cylinders with large-amplitude OOC involved using the trend-line in Figure 8 to estimate P_c* for an intact cylinder with the same level of OOC as the corroded specimen under consideration.

Experimental Curve A (dashed line) in Figure 9 was fit to test data for as-machined cylinders with general corrosion and small levels of OOC (gray diamonds), which were taken from [5,6]. A linear trend-line was used, despite the fact that the δ_c–λ_c relationship is likely nonlinear, because a meaningful nonlinear fit could not be achieved due to the limited δ_c-range that was studied and due to the experimental scatter.

The data for cylinders with large-amplitude OOC and in-phase corrosion (× symbols in Figure 9) fall on or above Curve A, suggesting that those cylinders were somewhat less affected by general corrosion damage than their nearly shape-perfect counterparts. That trend was predicted by the numerical models in [7] and was attributed to the effective increase in OOC due to corrosion, which is relatively greater for nearly shape-perfect hulls. Despite the apparent confirmation of results from [7], the experimental results must be interpreted cautiously due to the overlap in scatter between the groups of cylinders with small- and large-amplitude OOC and general corrosion.

Figure 9 shows that out-of-phase corrosion damage (white circles) may have only a small impact on collapse strength, even for severe cases of thinning. The evidence is convincing, despite the fact that only two cylinders had out-of-phase corrosion, since both test results fall above the trend-line and outside the scatter for the shape-perfect data. The numerical models in [7] predicted an increase in collapse pressure, compared to the intact case, with some combinations of out-of-phase corrosion and large-amplitude OOC. The experimental results were less extreme. Nonetheless, the tendency of tensile bending stresses caused by OOC to oppose compressive bending stresses resulting from corrosion, in combination with the effective reduction in OOC associated with the out-of-phase corrosion, nearly nullified the strength-reducing effects of the thinning in the experimental specimens. It is, however, important to reiterate that those benefits will diminish with decreasing OOC amplitude, so that, even if the true shape of an in-service hull is known, it cannot be assumed that out-of-phase corrosion damage is benign. Furthermore, although it has not been studied here, the difference between the effect of in-phase and out-of-phase corrosion on hulls failing by interframe collapse may be negligible.

4.2 COMPARISON OF CORROSION PITTING AND GENERAL CORROSION

The stress at a given corrosion pit would be expected to be affected by the location of the pit relative to other pits, as well as to the ring-stiffeners, and by the depth of corrosion. With complex pitting arrangements, such as the pattern used in these experiments, it is difficult to separate the relative influence of each of those factors. Nonetheless, the experimental data in Figure 4 show that corrosion pitting leads to the greatest stresses when the pits are in close proximity, when they are deep, and when they are located near the centre of a frame bay.

In Figure 9, the δ_c–λ_c data for specimens with pitting damage (black diamonds) are plotted with general corrosion damage data. The bounding area for the corrosion pitting was the same size as Patch C general corrosion. Since several cylinders with Patch C corrosion are included in Experimental Curve A, that curve represents an approximate baseline for general corrosion damage against which the effects of pitting damage can be compared.

All of the specimens with pitting fell on or above Curve A in Figure 9, although only one of the pitting results was outside the scatter of the general corrosion group. That suggests that an area of closely spaced corrosion pits is slightly less severe than an area of general corrosion with the same level of thinning and covering the area that bounds all of the pits. However, as with the discussion of in-phase general corrosion, the experimental trend is weak, and it can only be concluded that a large group of corrosion pits has an approximately

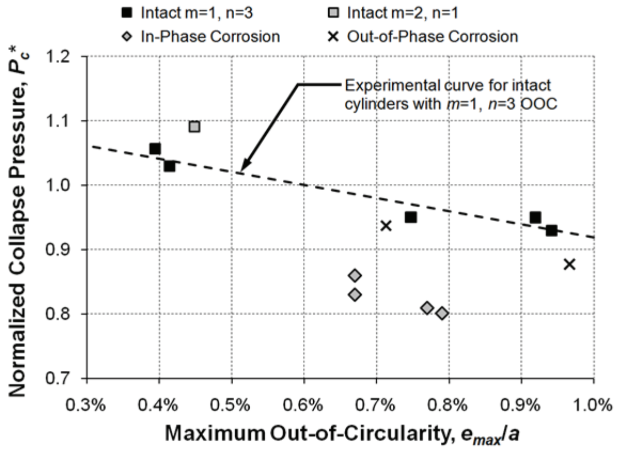

Figure 8: Normalized collapse pressure versus maximum OOC amplitude for cylinders with large-amplitude OOC.

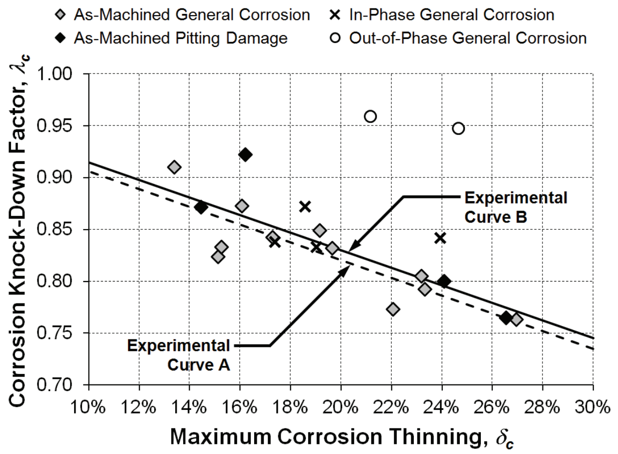

Figure 9: Corrosion knock-down factor, λ_c, as a function of the magnitude of shell thinning, δ_c, for specimens failing by overall collapse. Experimental Curve A is based on linear least squares regression of the data for as-machined specimens with general corrosion. Experimental Curve B is fit to the data for all specimens except those with out-of-phase general corrosion.

Table 4: Curve-fitting parameters for various data sets[a].

Figure	x	y	Data Set	m	b	r^2
Figure 8	e_{max}/a	P_c*	Intact	-20.4	1.12	0.93
Figure 9	δ_c	λ_c	Exp. Curve A	-0.86	0.99	0.72
Figure 9	δ_c	λ_c	Exp. Curve B	-0.85	1.00	0.63

Note: (a). Listing the slope, m, and intercept, (b) for the equation: $y = mx + b$. Curve fitting parameters are based on linear least squares regression of the indicated data set. The curve fit improves as r^2, the coefficient of determination, approaches unity.

equal effect on collapse strength as the same region covered by general corrosion of equivalent depth.

4.3 SUMMARY OF EXPERIMENTS

The δ_c–λ_c data in Figure 9 can be used to generate a corrosion knock-down curve for hulls with single cases of general corrosion, or multiple cases of pitting damage. Experimental Curve B (solid line in Figure 9) is based on linear least squares regression of all plotted data, except for those associated with out-of-phase corrosion (i.e. the white circles). The as-machined specimens and those with in-phase corrosion are lumped together since the effect of corrosion was found to be approximately independent of OOC magnitude. Specimens with out-of-phase corrosion are left out since they correspond with the best case scenario for a given level of thinning. Pitting damage was found to affect collapse strength in a similar manner as an equivalent area of general corrosion, and so specimens with those types of corrosion damage are also grouped together.

Curve B is slightly offset above Curve A, which is based on as-machined specimens with general corrosion. That difference is consistent with previous observations regarding the greater severity of general corrosion for otherwise shape-perfect cylinders, compared to corrosion pitting and general corrosion of cylinders with large-amplitude OOC. Based on Experimental Curve B, the percent reduction in overall collapse pressure is, on average, equal to 0.85 times the percent corrosion thinning. Curve B intercepts the vertical axis at λ_c=1, giving it some qualitative validation.

The experiments in [6] showed that the structural and material response of the aluminium test specimens are similar to real pressure hulls made of high-strength steel, and so the trends observed in the current experiments are applicable to real hulls. Nonetheless, the experimental curves in Figure 9 are not intended to be directly used for assessments of in-service corrosion damage since they are based on a limited range of parameters. Furthermore, those curves apply to overall collapse only, while the experiments in [5] showed that the effect of corrosion is related to the hull configuration and failure mode. The recommended approach to assessing in-service damage is to use numerical models that can account for the unique structural configuration, corrosion damage and out-of-circularity of the hull. Guidelines for capturing those features correctly in a numerical model, and producing the nonlinear collapse prediction, are presented in [9].

5. CONCLUSIONS

Corrosion thinning was found to impact overall collapse pressures through higher stresses in the damaged shell, and by changing the effective magnitude of out-of-circularity. In-phase corrosion patches that were preferentially aligned with the dominant out-of-circularity mode were found to be more detrimental to collapse strength than corrosion thinning that was out-of-phase with OOC. The scatter in experimental results was too great to confirm or reject the hypothesis that sensitivity to corrosion thinning diminishes with increasing OOC.

The current work highlights the importance of the interaction of corrosion damage with the actual shape of the pressure hull. When assessing corrosion damage to real submarines, it is necessary to model the true shape of the hull, and the correct location of the thinning with respect to that shape.

Corrosion pitting was found to be most severe when the pits are clustered close together near the centre of a frame bay. A group of pits is approximately equivalent to an area of general corrosion, although pitting damage is less severe, to an extent that depends on the spacing between pits. It is difficult to precisely quantify the difference based on the experiments, due to the level of scatter, but numerical models could be used to extend the experimental study. Nonetheless, structural assessments of real pressure hulls with pitting damage, whereby a group of pits is treated as an equivalent area of general corrosion, are not excessively conservative.

6. ACKNOWLEDGEMENTS & COPYRIGHT

The experiments described in this paper were a joint project of the Netherlands Ministry of Defence and the Department of National Defence of Canada.

The authors would like to thank their many colleagues in the Netherlands and Canada who have contributed to the experimental program.

8. REFERENCES

1. SMITH, M. J., 'Structural Modelling and Strength Assessment of the Victoria-class Submarine Pressure Hull', *Maritime Engineering Journal, Fall 2005, pp 9-13.*

2. BAYLEY, C. and MACKAY, J., 'Strategic Research Agenda: Verification and Validation of Numerical Welding Approaches', *DRDC Atlantic TM 2009-170, Defence R&D Canada - Atlantic*, 2009.

3. 'SSP74: Design of Submarine Structures', *Sea Systems Publication 74, Defence Procurement*

Agency, United Kingdom Ministry of Defence, 2001.

4. MACKAY, J. R., SMITH, M. J. and PEGG, N. G., 'Design of pressure hulls using nonlinear finite element analysis', *Proceedings of the 25th International Conference on Offshore Mechanics and Arctic Engineering, Paper No. OMAE2006-92591, ASME, Hamburg*, 2006.
5. MACKAY, J. R., SMITH, M. J., VAN KEULEN, F., BOSMAN, T. N. and PEGG, N. G., 'Experimental investigation of the strength and stability of submarine pressure hulls with and without artificial corrosion damage', *Marine Structures, Volume 23, pp 339-359*, 2010.

6. MACKAY, J. R. and VAN KEULEN, F., 'The Sensitivity of Overall Collapse of Damaged Submarine Pressure Hulls to Material Strength', *Journal of Offshore Mechanics and Arctic Engineering, in press, DOI 10.1115/1.4007051*, 2012.

7. SMITH, M. J. and MACKAY, J. R., 'Overall elasto-plastic collapse of ring stiffened cylinders with corrosion damage', *Transactions of the Royal Institution of Naval Architects Part 1A – International Journal of Maritime Engineering, Volume 147, pp 53-61,* 2005.

8. KENDRICK, S.B., 'The influence of shape imperfections and residual stresses on the collapse of stiffened cylinders', *Conference on Significance of Deviations from Design Shape, pp 25-35*, 1979.

9. MACKAY, J. R., JIANG, L. And GLAS, A. H., 'Accuracy of nonlinear finite element collapse predictions for submarine pressure hulls with and without artificial corrosion damage', *Marine Structures, Volume 24, pp 292-317,* 2011.

10. MACKAY, J. R., 'Experimental investigation of the strength of damaged pressure hulls – Phases 5 & 6: The influence of out-of-circularity on collapse', *DRDC Atlantic TM 2010-239, Defence R&D Canada - Atlantic*, 2011.

11. MACKAY, J. R., 'Experimental investigation of the strength of damaged pressure hulls – Phase 7: The interaction of multiple corrosion damage cases', *DRDC Atlantic TM 2011-034, Defence R&D Canada - Atlantic*, 2011.

12. HIBBELER, R. C., 'Mechanics of Materials, Third Edition', *Prentice Hall Canada, Inc., Toronto,* 1997.

13. MACKAY, J. R. and VAN KEULEN, F., 'A review of external pressure testing techniques for shells including a novel volume-control method', *Experimental Mechanics, Volume 50, pp 753-772*, 2010.